Aerosol Science and Technology
Publication details, including instructions for authors and subscription information:
http://www.tandfonline.com/loi/uast20

Evaluation of a Method for Measurement of the Concentration and Size Distribution of Black Carbon Particles Suspended in Rainwater

Sho Ohata [a], Nobuhiro Moteki [a] & Yutaka Kondo [a]

[a] Department of Earth and Planetary Science, Graduate School of Science, The University of Tokyo, Tokyo, Japan

Available online: 08 Jun 2011

To cite this article: Sho Ohata, Nobuhiro Moteki & Yutaka Kondo (2011): Evaluation of a Method for Measurement of the Concentration and Size Distribution of Black Carbon Particles Suspended in Rainwater, Aerosol Science and Technology, 45:11, 1326-1336

To link to this article: http://dx.doi.org/10.1080/02786826.2011.593590

Aerosol Science and Technology, 45:1326–1336, 2011

ISSN: 0278-6826 print / 1521-7388 online
DOI: 10.1080/02786826.2011.593590

Evaluation of a Method for Measurement of the Concentration and Size Distribution of Black Carbon Particles Suspended in Rainwater

Sho Ohata, Nobuhiro Moteki, and Yutaka Kondo

Department of Earth and Planetary Science, Graduate School of Science, The University of Tokyo, Tokyo, Japan

We make detailed evaluations of a method of measuring the mass concentration and size distribution of black carbon (BC) particles suspended in water for the purpose of application to rainwater samples. Water samples were aerosolized with an ultrasonic nebulizer. Generated water droplets were dried in order to extract airborne BC particles. The mass of each BC particle was then measured by a Single Particle Soot Photometer (SP2), based on the laser-induced incandescence technique. Under the optimized operating conditions of our measurement system, the overall efficiency of the extraction of BC particles from rainwater was determined to be 11.4% ± 0.83% by mass, resulting in a total uncertainty of about ±20% for the measurement of the BC concentration in rainwater. The change in efficiency due to water-soluble species was found to be negligibly small for rainwater samples analyzed in this study. The determination of the efficiency by using standard BC solutions was necessary at an appropriate frequency because changes in the overall conditions of the system lead to changes in the efficiency in the long term. The size of BC particles in rainwater can be overestimated because of the coagulation of BC particles in the process of extraction by the nebulizer. This effect increased with the increase in BC concentration in rainwater. The effect can be minimized by dilution of rainwater samples by pure water. The volume of a rainwater sample required for BC measurement was less than 5 mL, enabling measurement for weak rain or highly time-resolved measurements during each rain event.

Received 30 September 2010; accepted 29 May 2011.

We thank T. Kogawa for his assistance with the field measurements. We also thank T. Miyakawa for great advice and assistance with the laboratory experiments. This work was supported by the Ministry of Education, Culture, Sports, Science, and Technology (MEXT), the strategic international cooperative program of the Japan Science and Technology Agency (JST), and the global environment research fund of the Japanese Ministry of the Environment (A-1101).

Address correspondence to Yutaka Kondo, Department of Earth and Planetary Science, Graduate School of Science, The University of Tokyo, Hongo 7-3-1, Bunkyo-ku, Tokyo, 113-0033, Japan. E-mail: kondo@eps.s.u-tokyo.ac.jp

1. INTRODUCTION

Black carbon (BC) is produced by incomplete combustion of fossil fuels and biomass. It effectively absorbs solar radiation and warms the atmosphere on regional and global scales (IPCC [Intergovernmental Panel on Climate Change] 2007; Ramanathan et al. 2007). Deposition of BC onto snow and ice has potential to change the surface albedo (Warren and Wiscombe 1980; Clarke and Noone 1985), contributing to warming of the Arctic (Hansen and Nazarenko 2004; Flanner et al. 2007, 2009). Distributions of BC are controlled by emissions, transport, and deposition during transport. Wet deposition has been observed to strongly control the efficiency of BC transport from the planetary boundary layer (PBL) to the free troposphere (FT; Matsui et al. 2011; Kondo et al. 2011b).

Spatial and temporal variations of the deposition flux of BC are controlled by a series of complex processes. First, freshly emitted BC particles from fossil fuel sources are hydrophobic. However, they become active as cloud condensation nuclei (CCN) by their coating with hygroscopic materials (Dusek et al. 2006; Kuwata et al. 2007, 2009). The CCN activity of BC particles is controlled by their size and mixing state. Under super-saturation conditions of water vapor, aged BC particles are activated into cloud droplets. Depending on the liquid water content available, the formed droplets grow into raindrops followed by precipitation. The transport efficiency of BC has been observed to decrease with the amount of precipitation that air masses experience during transport from the PBL to the FT (Matsui et al. 2011; Kondo et al. 2011b). Below-cloud scavenging of aerosols with diameters of 0.05–1 μm by falling raindrops is not efficient (Slinn 1983; Seinfeld and Pandis 2006), the so-called Greenfield gap. These complex processes are not fully understood, however, due to a lack of appropriate observations.

The BC concentration in rainwater is a useful parameter to understand the overall processes of wet deposition of BC. Mass concentrations of BC were detected in rainwater in tropical regions (Ducret and Cachier 1992) and at mid-latitudes (Ogren et al. 1984; Chylek et al. 1999; Cerqueira et al. 2010).

Total mass concentrations of BC in rainwater were measured by a thermal-optical-transmittance (TOT) technique (Ogren and Charlson 1983; Hadley et al. 2008). BC particles extracted from rainwater were thermo chemically converted into CO_2, which can be quantified by infrared absorption.

As discussed above, the CCN activity of BC particles is strongly influenced by the microphysical properties of BC. Therefore, the measurement of the size distribution of BC particles suspended in rainwater should greatly improve the understanding of the microphysical processes of activation of BC-containing particles as CCN and uptake into cloud droplets. They are useful in validating the wet deposition flux calculated by size and mixing state resolved three-dimensional models used for assessing impacts of BC on climate (Jacobson 2001; Stier et al. 2005, 2006; Kajino and Kondo 2011). However, the number size distribution of BC in rainwater has not been reported thus far.

In order to achieve this, we essentially used the same methodology developed for the measurements of BC concentration in ice core by McConnell et al. (2007). Namely, BC particles suspended in water were aerosolized by an ultrasonic nebulizer, followed by the measurement of the mass of each extracted BC particle by a Single Particle Soot Photometer (SP2). The quantitative interpretation of the data derived by this method requires a full assessment of possible errors. However, up to now, no detailed evaluations of the uncertainties of this method have been reported, despite complex physico-chemical processes occurring in water and in extracting BC particles from water.

The purpose of this study is to quantify errors associated with each step taken in finally deriving the BC concentration in water. The critical points we identified and quantify are (1) the stability of BC mass concentrations during storage of a rainwater sample, (2) the efficiency of extracting BC from rainwater by the nebulizer, (3) the effect of dissolved chemical compounds on the extraction efficiency, and (4) possible changes in the BC size distribution during evaporation of water droplets containing BC particles. On the basis of these evaluations, we also show examples of the measurements of BC size distribution in rainwater collected in Tokyo for the first time.

2. LABORATORY EXPERIMENTS

Figure 1 shows the experimental setup used for this study. Water samples containing BC particles are transferred to an ultrasonic nebulizer (U-5000AT, Cetac Technologies Inc., Omaha, Nebraska, USA) by a peristaltic pump (REGRO Analog, ISMATEC SA., Feldeggstrasse, Glattbrugg, Switzerland) at a calibrated flow rate. Figure 2 shows an expanded diagram of the U-5000AT nebulizer.

Sample water is fed to a piezoelectric transducer by a peristaltic pump. Some fraction of the introduced water is converted to small droplets on the surface of the piezoelectric transducer, which oscillates at a frequency of 1.4 MHz. The portion of

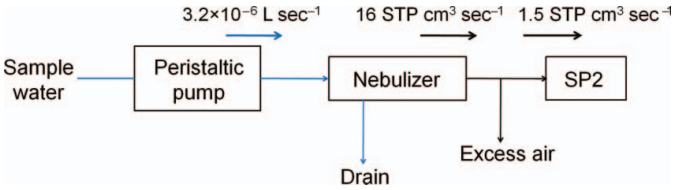

FIG. 1. Schematic diagram of the experimental setup for measuring BC particles in rainwater. (Color figure available online.)

the water sample not aerosolized by this process is removed through the first drain. Dry, clean air at a flow rate of 16 $cm^3\ s^{-1}$ at standard temperature and pressure (STP) is introduced near the transducer to produce an airflow. Downstream of the transducer, the water droplets are dried while passing through a tube heated at 140°C, generating a mixture of BC particles and water vapor molecules. Water vapor is removed through condensation onto a tube cooled at 3°C. The condensed water is taken out of the nebulizer through the second and third drains. By evaporation of droplets, BC particles or other types of residue particles are released into the atmosphere.

These dried particles are introduced to the SP2 at a flow rate of 1.5 $cm^3\ s^{-1}$ STP. The mass and mixing state of individual BC particles are analyzed by the SP2. Detailed descriptions of the SP2 have been given elsewhere (Moteki and Kondo 2007, 2010). In brief, visible incandescent light is emitted from BC particles heated to ∼4000 K in a laser beam. The peak signal of the laser-induced incandescence (LII) detected by photomultiplier tubes is related to the mass of ambient BC particles. The calibration methods using ambient BC and fullerene soot have been described elsewhere (Moteki and Kondo 2010; Kondo et al. 2011a). The size range of BC covered by the SP2 is between 70 and 850 nm.

Two avalanche photodiodes are used to detect light signals scattered by the particles. The peak scattering signal is converted to the scattering cross section of the particles. Calibration is performed using polystyrene latex (PSL) spheres with a refractive index of 1.59 + 0i (Kondo et al. 2011b).

In order to determine the fraction of BC particles in water extracted by the nebulizer, we used Aqua Black 001 (AB-001) and Aqua Black 162 (AB-162; TOKAI Carbon Co., LTD, Tokyo, Japan) as laboratory standards of BC suspended in water. BC particles in AB-001 and AB-162 were stably dispersed in water without sedimentation or coagulation, because the surface of individual BC particles was functionalized by carboxyl groups to increase their hydrophilicity. We determined the mass fractions of solid BC particles in AB-001 and AB-162 samples to be 20.2% ± 0.6% and 19.7% ± 0.6%, respectively, by drying AB-001 and AB-162 with known volumes, followed by measurements of the masses of solid residues after drying.

We controlled the BC mass concentrations of AB-001 and AB-162 used for the experiments by dilution with pure water. The determination of BC mass by the SP2 requires a calibration

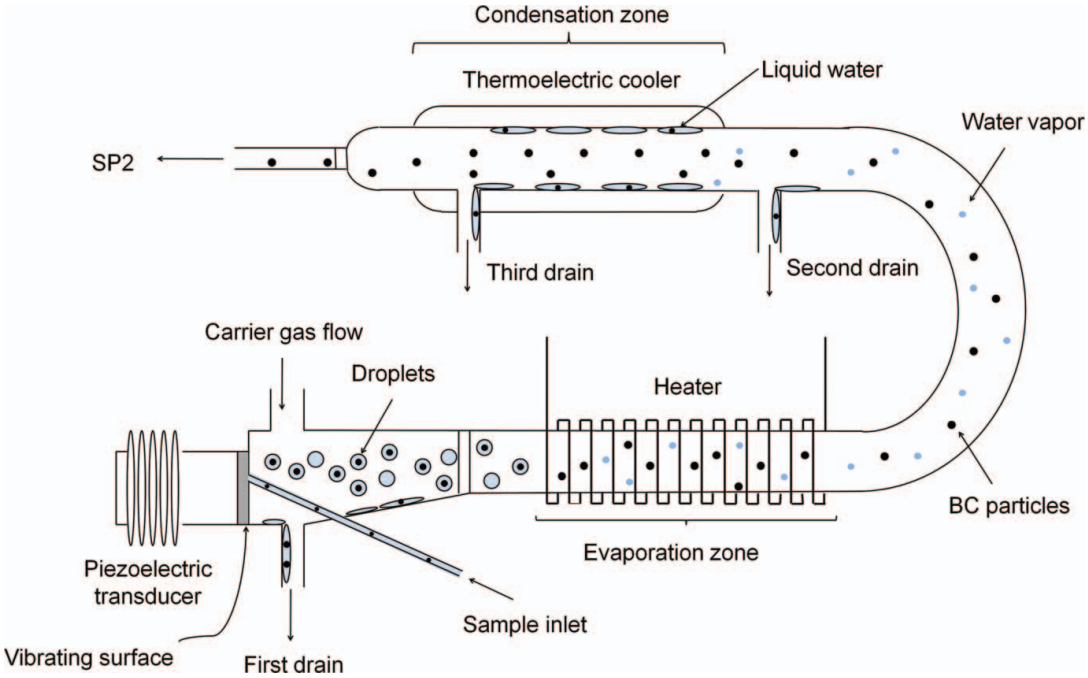

FIG. 2. Expanded diagram of the ultrasonic nebulizer (U-5000AT). (Color figure available online.)

curve depending on the types of BC samples because LII signals depend, in part, on the refractive index and shape of BC (Moteki and Kondo 2010). For the measurements of AB-001 and AB-162, we used the corresponding calibration curves of these laboratory samples. On the other hand, we used the calibration curve of fullerene soot (Alfa Aesar Inc., Stock#40971, Lot#FS12S011 Alfa Aesar Inc., Massachusetts, USA) for measurements of BC particles in rainwater by the SP2. The relationship between the LII signal and BC mass of fullerene soot was similar to that of ambient soot sampled in Tokyo (Moteki and Kondo 2010). Each sample of aqueous dispersion of BC in a bottle was stirred in an ultrasonic bath for 15 min to homogenize the BC concentration inside the bottle. We determined the efficiency (ε) of BC extraction from the BC mass concentration in airflow measured by the SP2 and the BC mass concentration in water:

$$\varepsilon = M_{SP2}\, F_{neb}/(m_{samp}\, V_{pump}), \qquad [1]$$

here M_{SP2} is the BC mass concentration measured by the SP2 (μg cm^{-3}), F_{neb} is the nebulizer gas flow rate (cm^3 s^{-1}), m_{samp} is the sample BC mass concentration (μg L^{-1}), and V_{pump} is the liquid flow rate of the pump (L s^{-1}). As shown in the next section, size distributions of BC particles were well fitted by a lognormal distribution function. We assumed that the BC size distribution is approximated by a lognormal distribution function throughout this study. The mass of BC particles smaller than the SP2 detection limit, which is approximately 70 nm, was estimated by the extrapolation of the lognormal function. By using the measured value of ε, we determined the BC mass concentration in a rainwater sample by the following equation:

$$m_{samp} = M_{SP2}\, F_{neb}/(\varepsilon V_{pump}). \qquad [2]$$

3. NEBULIZER EFFICIENCY

3.1. Measurements Using Pure Water

The efficiency (ε) was determined by using a water solution of AB-001 and AB-162 at different BC mass concentrations. For this measurement, F_{neb} and V_{pump} were set to 16.4 cm^3 s^{-1} STP and 3.16 $\times$ 10^{-6} L s^{-1}, respectively. Figure 3 shows the mass size distributions of AB-001 and AB-162 versus mass equivalent diameter (D_{BC}).

We assumed a true density of BC of 2.0 g cm^{-3} to convert the measured BC mass to D_{BC}. The curves fitted by lognormal distribution functions are also shown. Each size distribution was obtained by averaging continuous measurements for 10 min. The fitting error of the mass median diameter (MMD) was less than 3 and 1 nm for AB-001 and AB-162, respectively. The measurements, repeated for 3 days, showed that the measured MMD was stable to within 2%, demonstrating the stability of the measurement system during this period. The fraction of BC mass directly detected by the SP2 was estimated to be 64% $\pm$ 2% and 83% $\pm$ 1% for AB-001 and AB-162, respectively. The unmeasured BC mass was accounted for in deriving the total BC mass concentrations (M_{SP2}).

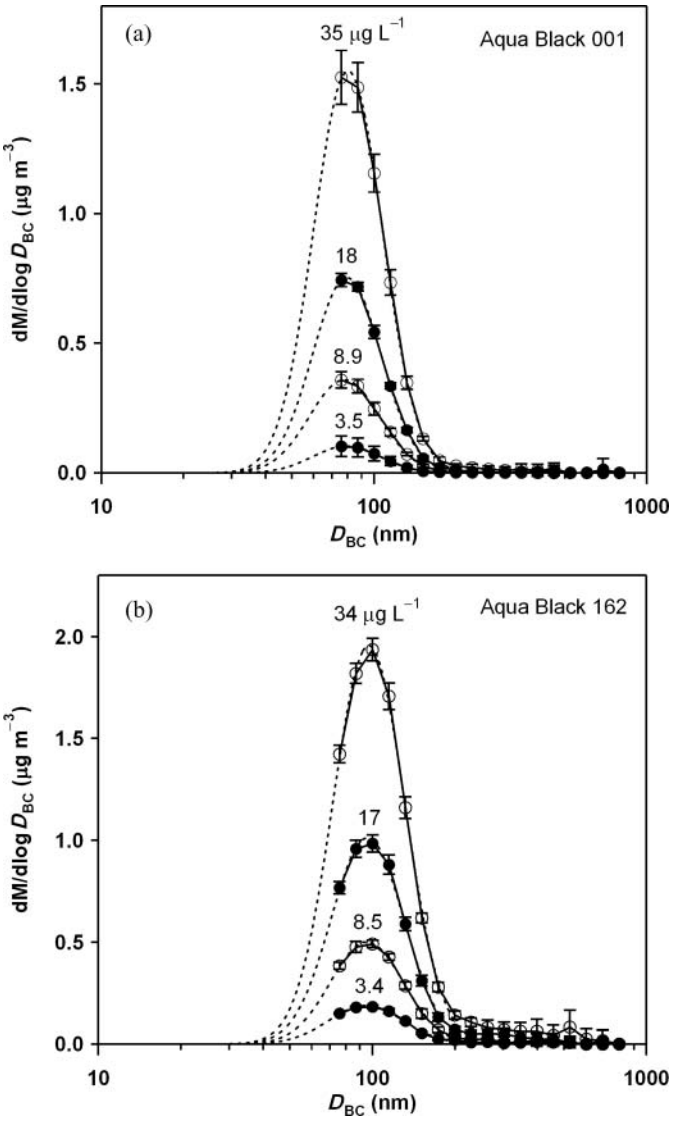

FIG. 3. Mass size distributions of (a) Aqua Black 001 and (b) Aqua Black 162. Approximately 36% and 17% of the BC particle mass were not detected by the SP2 (BC < 70 nm) for AB-001 and AB-162, respectively. Bars indicate 1 σ values.

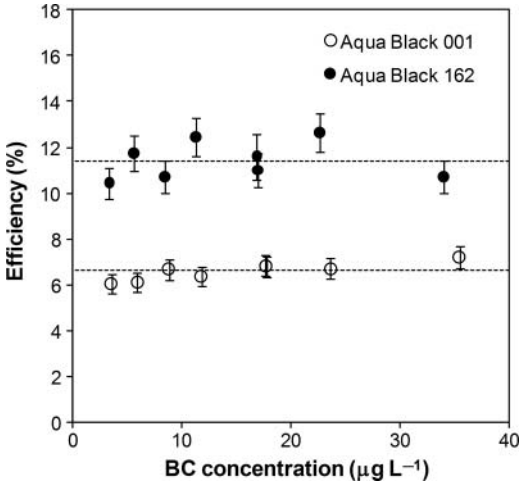

FIG. 4. Efficiencies of the nebulizer in extracting BC measured as a function of BC mass concentration in water. Dashed lines show the average values. Bars indicate 1 σ values of each data.

We derived the values of ε for different m_{samp} according to Equation (1). Figure 4 shows that the value of ε depended little on m_{samp}.

The average ε values were 6.59% $\pm$ 0.38% and 11.4% $\pm$ 0.83% for AB-001 and AB-162, respectively. As shown in Figure 3, the unmeasured BC mass fraction of AB-001 was larger than that of AB-162. In particular, the uncertainty of the smallest size bin of AB-001 can substantially alter the fitted distribution and the value of estimated M_{SP2}. For instance, the AB-001 mass fractions measured by the SP2 were 46% and 78% when the fitted size distribution was shifted to smaller and larger diameters by 10 nm, the width of the smallest size bin, respectively. In the same way, AB-162 mass fractions were calculated to be 73% and 91%, respectively. Therefore, potential uncertainty of the efficiency (ε) of AB-001 is much larger than that of AB-162 even though it was not included in the error bars in Figure 4.

In addition to the larger potential errors in ε for AB-001, there were some inconsistencies in the analysis of the size distributions using AB-001, as discussed in Section 5.2. Considering these, we used an efficiency $\varepsilon = 11.4\% \pm 0.83\%$, determined for AB-162 for BC measurements in rainwater samples. Hoenig et al. (2000) reported the efficiency (ε) of the same ultrasonic nebulizer to be 9.1% for measurements of some trace elements by inductively coupled plasma—atomic emission spectrometry (ICP-AES), consistent with the present determination.

The ε of about 11% indicates that 89% of the mass of injected BC particles was lost by the nebulizer. Approximately 19% of the volume of the sample water was removed at the first drain without conversion into water droplets at the piezoelectric transducer. We assumed that the same fraction (19%) of BC mass introduced to the nebulizer was lost by this step. The remaining 81% of the BC mass was aerosolized and transported downstream. Considering that about 11% of the BC mass was measured by the SP2, the remaining 70% (= 100% − 11% − 19%) of the BC mass was likely deposited on the walls of the tubing or lost at the second and third drains. The fraction of the BC mass lost by the nebulizer depends on the configuration of the nebulizer and its performance. As shown in Figure 2, the nebulizer used in this study consists of a piezoelectric transducer, 3 drains, and a curved tube with a heater and cooler, all of which would have effects on the loss of BC. It should be noted that the ε of about 11% depends on the overall conditions of our system, and the value of ε derived in this study is not directly applicable to other measurement systems.

The liquid flow rate of the pump (V_{pump}) was found to be another important factor in controlling ε. Figure 5 shows the measured ε versus V_{pump}.

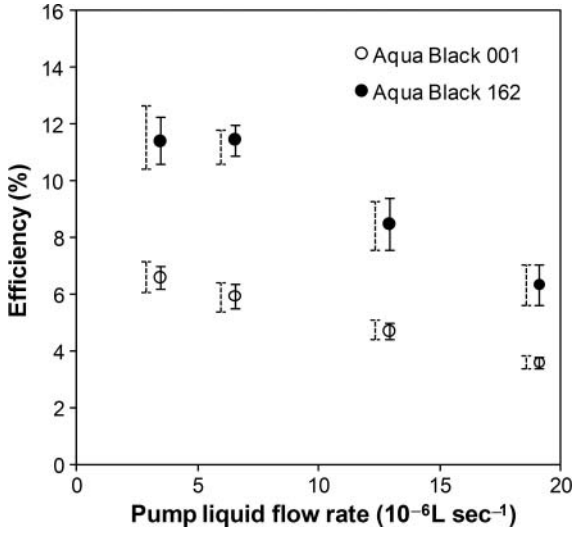

FIG. 5. Efficiencies of the nebulizer for Aqua Black 001 and Aqua Black 162 as a function of the liquid flow rate of the peristaltic pump. Open and closed circles stand for the average values. Dashed and solid bars indicate the range of the data and 1 σ values, respectively.

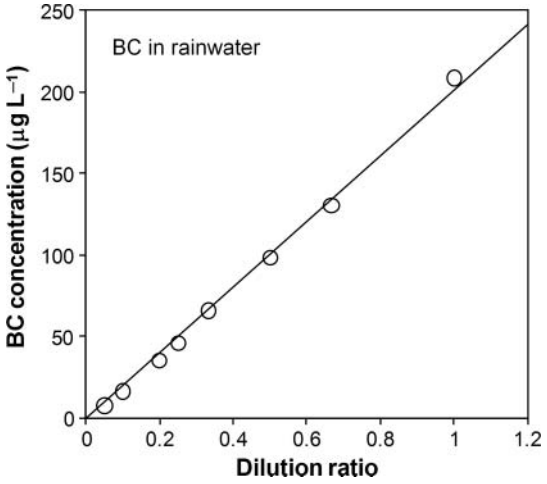

FIG. 6. Measured BC concentration in rainwater versus dilution ratio. The solid line indicates linear fitting.

The values of ε decreased with the increase in V_{pump}. This suggests that the fraction of the volume of water that was aerosolized on the vibrating surface decreased with the increase in the volume of sample water. Waite and Ramsden (1971) also reported a similar dependence of ε on V_{pump} for a different kind of apparatus including an ultrasonic nebulizer. The ε values were relatively stable at a V_{pump} of about 3–7 $\times$ 10^{-6} L s^{-1}.

For this study, we chose a V_{pump} of 3.2 $\times$ 10^{-6} L s^{-1} to maintain stable values of ε. However, the long-term stability of ε is not obvious, partly due to the dependence of ε on V_{pump} and due to other unknown factors not investigated by this study. In fact, we remeasured ε 6 months after the first determination of ε. The value of ε was 8.0% $\pm$ 1.0%, 30% lower than the previous value of 11.4%. Determination of ε by a standard BC solution is necessary for every analysis period of BC in rainwater in order to maintain the overall accuracy, especially considering that ε is much lower than 100%.

3.2. Effect of Water-Soluble Species

In rainwater, various chemical species, including inorganic (typically sulfate, nitrate, and ammonium) and water-soluble organic species, are dissolved, coexisting within dispersed BC particles (Willey et al. 2000; Okuda et al. 2005). These water-soluble species may affect the surface tension of the rainwater. The number and size of droplets generated at the piezoelectric transducer and resulting nebulizer efficiency may change, possibly by changes in the surface tension of rainwater caused by coexisting water-soluble species.

Humic-like substances (HULIS) are known to be surface active, and the effect of Suwannee River Fulvic Acid (SRFA; one of the HULIS compounds) on surface tension was quantified by laboratory experiments (Kiss et al. 2005; Svenningsson et al. 2006). Facchini et al. (2000) observed about a 15%–20% decrease in surface tension of wet aerosol and fog samples at concentrations of water-soluble organic carbon (WSOC) of about 100 mg L^{-1}, compared with the surface tension of pure water. The concentrations of dissolved organic carbon (DOC) in rainwater collected in Tokyo in the winter and summer seasons of 1992 were reported to be in the range of 1–23 mg L^{-1} (Sempere and Kawamura 1994).

In order to assess the effect of water-soluble species on the nebulizer efficiency, we first measured changes of BC concentrations in rainwater by dilution with pure water by a factor of 10. Rainwater was collected on the campus of the Research Center for Advanced Science and Technology (RCAST), the University of Tokyo, Tokyo, on December 21, 2010. The BC concentration in this sample was measured to be as high as 208 μg L^{-1}. High BC concentrations were often observed at the initial phase of precipitation in Tokyo. The atmospheric WSOC/BC ratios typically ranged between about 1/3 and 1 in Tokyo in winter (Miyazaki et al. 2006).

Figure 6 shows the measured BC concentrations in rainwater versus the dilution ratios.

The measured BC concentration was nearly proportional to the dilution ratio. This demonstrates no detectable effects of water-soluble species on ε for this rainwater sample. It should be noted that the BC concentration was one of the highest values measured in Tokyo and likely represents the highest concentrations of DOC there as well. The changes in the size distribution of BC by dilution are discussed in Section 5.2.

In addition to the dilution method, we also estimated the dependence of ε on water-soluble species by adding ammonium sulfate [$(NH_4)_2SO_4$] and SRFA to sample rainwater, which should have already contained an unknown amount of water-soluble species. The rainwater we used was collected in Cape Hedo in Okinawa, a remote site located in East China Sea, on June 10, 2010, and the BC concentration was measured to be

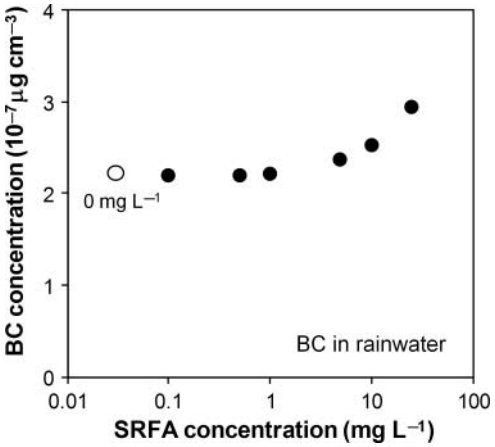

FIG. 7. BC concentrations in airflow measured by the SP2 versus SRFA concentration added to the rainwater sample.

16.2 μg L^{-1}, because the rainwater sampled in Tokyo was totally consumed for the analysis.

We chose concentrations of $(NH_4)_2SO_4$ and SRFA to be in the range of 0.1–100 and 0.1–25 mg L^{-1}, respectively. This range of $(NH_4)_2SO_4$ concentration covers the typical values in rainwater observed in Japan. For example, Okuda et al. (2005) showed that the mean concentrations of NH_4^+ and SO_4^{2-} at the 9 sampling sites in the Tokyo metropolitan area between June 1990 and May 2002 were about 0.7 and 2.4 mg L^{-1}, respectively. The SRFA concentration of 0.1–25 mg L^{-1} covers the range of DOC concentrations measured in Tokyo (1–23 mg L^{-1}), discussed above.

Figure 7 shows the airborne BC concentrations extracted by the nebulizer versus the concentrations of SRFA added to the rainwater sample.

The effect of dilution of the sample due to the addition of SRFA was taken into account in deriving the BC concentrations. At SRFA concentrations below 1 mg L^{-1}, the measured BC concentration was stable at about 2.2×10^{-7} μg cm^{-3}. The BC concentration increased by 14% and 32% at SRFA concentrations of 10 and 25 mg L^{-1}, respectively. These results suggest that the efficiency increases only at very high concentrations of HULIS, possibly due to the decrease in the surface tension of the sample water. The stability of the efficiency at lower SRFA concentrations is consistent with the results obtained by dilution with pure water.

For the $(NH_4)_2SO_4$ concentrations between 0.1 and 100 mg L^{-1}, the extracted BC concentrations were stable to within ±6.3%. This indicates no detectable interference by $(NH_4)_2SO_4$.

Not all the DOC should be composed of HULIS. In addition, the inclusion of soluble species into cloud droplets will be quite different from the simple addition of specified compounds in the laboratory. We consider that dilution of rainwater samples with pure water provides the most robust estimate of the overall effect considering the complexity of the chemical and physical processes involved. Therefore, we conclude that errors due to possible changes in surface tension are negligible (less than about 5%) for the analysis of rainwater samples used in this study. However, under the conditions of much higher HULIS concentrations, we may need to consider this effect. Even in such cases, the effect can best be estimated by diluting samples, without requiring chemical analysis of water-soluble species.

The typical errors of ε, M_{SP2}, F_{neb}, and V_{pump} were estimated to be about 15%, 10%, 5%, and 5%, respectively, based on the assumption of the negligible effect of water-soluble species on ε and the repeated measurement of ε, M_{SP2}, F_{neb}, and V_{pump}. The overall uncertainty of measurement of the BC concentration in rainwater (m_{samp}) was calculated to be about ±20%.

4. STABILITY OF BC DURING STORAGE

Rainwater samples need to be stored in a refrigerator before analysis in the laboratory, although the period of storage may change depending on various factors. Therefore, we assessed possible changes in BC mass concentrations during typical storage periods. For this purpose, rainwater was collected in Tokyo on October 9, 2010.

We first measured the reproducibility of the analysis of the same sample within a few hours. Just before the analysis, we stirred the sample in an ultrasonic bath for 30 min to avoid loss of BC particles onto the walls of the glass bottles. Figure 8 shows a time series of BC mass concentrations measured by the SP2 continuous nebulization of this rainwater sample for about 100 min.

Each data point stands for a 10-min average of the BC concentrations. Each analysis consumes approximately 1.9 mL rainwater sample. The BC concentrations were stable to within 2.4% relative standard deviation.

Next, the long-term stability of the rainwater sample stored in a refrigerator was assessed by repeating the measurement of the same rainwater sample on different days. Figure 9 shows

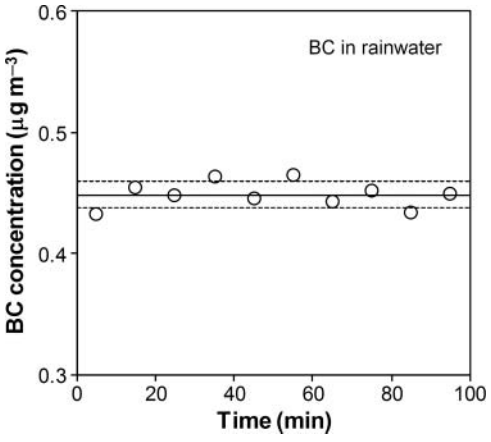

FIG. 8. Changes in the BC mass concentration measured by the SP2 for about 100 min. The solid line and dashed lines stand for the average and 1 σ values, respectively.

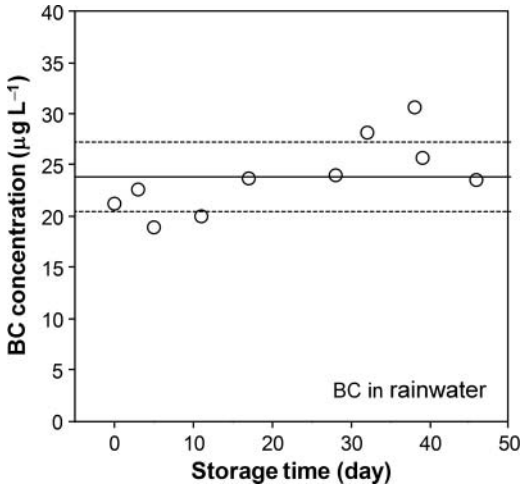

FIG. 9. Measured BC concentrations in rainwater during storage of a few months. The solid line and dashed lines stand for the average and 1 σ values, respectively.

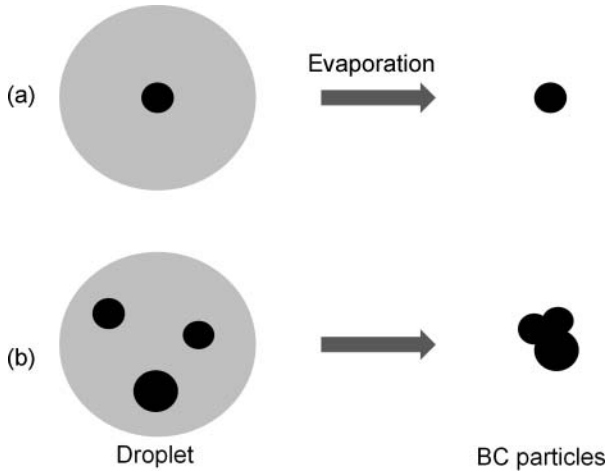

FIG. 10. Expanded view of the process of evaporation of droplets containing (a) single BC particle and (b) multiple particles.

the BC concentration versus the time of sample storage, up to 50 days.

The variability of the measured BC mass concentration was to within14%. A slight increase in the BC mass concentration with storage time might have been due to the evaporation of water, especially by stirring the same sample in an ultrasonic bath for each analysis. This result indicates that the rainwater sample was stable over a month to within about 15%.

5. CHANGES IN BC SIZE IN THE NEBULIZER

5.1. PSL and Aqua Black

We assessed possible changes in the sizes of BC particles in the nebulizer. Figure 10 shows a schematic diagram of the mechanism of changes in BC particle diameters through coagulation upon evaporation of water droplets in the nebulizer.

The evaporation occurs in the heated evaporation zone, shown in Figure 2. Each droplet contains either a single BC particle [case (a)] or multiple BC particles [case (b)]. For case (a), the size distribution of generated airborne BC particles is the same as that in the water sample. In contrast, for case (b), the size distribution of BC particles shifted to larger sizes as compared with that in the water sample. The magnitude of this effect is anticipated to increase with the increase in BC concentration in water.

We assessed the effect of coagulation by laboratory measurements using aerosol with known diameters. For this purpose, we used mono-disperse PSL, Aqua Black, and BC in rainwater.

First, the measurements were made using PSL with known diameters (202, 294, and 402 nm). We prepared water suspensions of PSL particles with number concentrations close to the maximum BC concentrations in rainwater collected in Tokyo in 2009 and 2010. The concentrations of the prepared PSL particles and the measured BC concentrations are summarized in Table 1.

We measured the number and volume size distributions of the airborne PSL particles by the SP2. Table 2 summarizes the ratios of the number of doublets or triplets to the total number of PSL particles detected by the SP2.

The fractions of the measured doublets or triplets were about 10% at diameters of 202 and 294 nm and close to zero at 402 nm.

TABLE 1
Sample water used in this study. Rainwater samples were collected at the University of Tokyo campus in December 2009 and in October and December 2010 and at Cape Hedo in Okinawa in June 2010. BC mass concentrations in rainwater samples were determined by the efficiency shown in Section 3

Sample name	Sample number	BC mass concentration in sample water (μg L^{-1})	PSL or BC number concentration after nebulization (STP cm^{-3})	BC mass concentration after nebulization (STP μg cm^{-3})
AB-001	8	3.5–35		4.1×10^{-8}–4.9×10^{-7}[a]
AB-162	8	3.4–34		6.8×10^{-8}–6.9×10^{-7}[a]
PSL	3		PSL: 4.5×10^{2}–6.6×10^{2}	
Rainwater	9	9–208	BC: 6.1 × 10–7.9×10^{2}[a]	1.6×10^{-7}–3.0×10^{-6}

[a]Considering the detection limit of the SP2, these values were modified by fitting their size distributions by lognormal functions.

TABLE 2
Ratios in number and mass concentrations of doublets or triplets of PSL particles to the total PSL particles measured by the SP2

Diameter (nm)	Number ratio (%)	Mass ratio (%)
202	11	18
294	10	19
402	1	2

This result suggests that coagulation can increase the size of BC during the evaporation of droplets, depending on particle concentration.

Second, we made more detailed investigations of this effect by using Aqua Black particles. The size distributions of AB-001 and AB-162 samples were obtained by experiments to determine ε, as discussed in Section 3 (Figure 3). The MMD and geometric standard deviations for mass size distributions (σ_{gm}) were derived for the lognormal fitted size distributions. These parameters are plotted versus BC concentration in water in Figure 11.

The MMD and σ_{gm} values increased and decreased with the increase in BC concentration, respectively. The opposite changes in MMD and σ_{gm} are consistent with the interpretation of the effect of BC coagulation, as suggested by the PSL experiments. The slopes of the fitted lines to the MMD and σ_{gm} data are summarized in Table 3.

Count median diameters (CMD) and geometric standard deviations for number size distributions (σ_{gc}) of AB-001 and AB-162 particles were not measured by the SP2 due to its detection limit for BC size. The observed BC mass concentrations in rainwater were comparable with the range of mass concentrations shown in Figure 3, as summarized in Table 1.

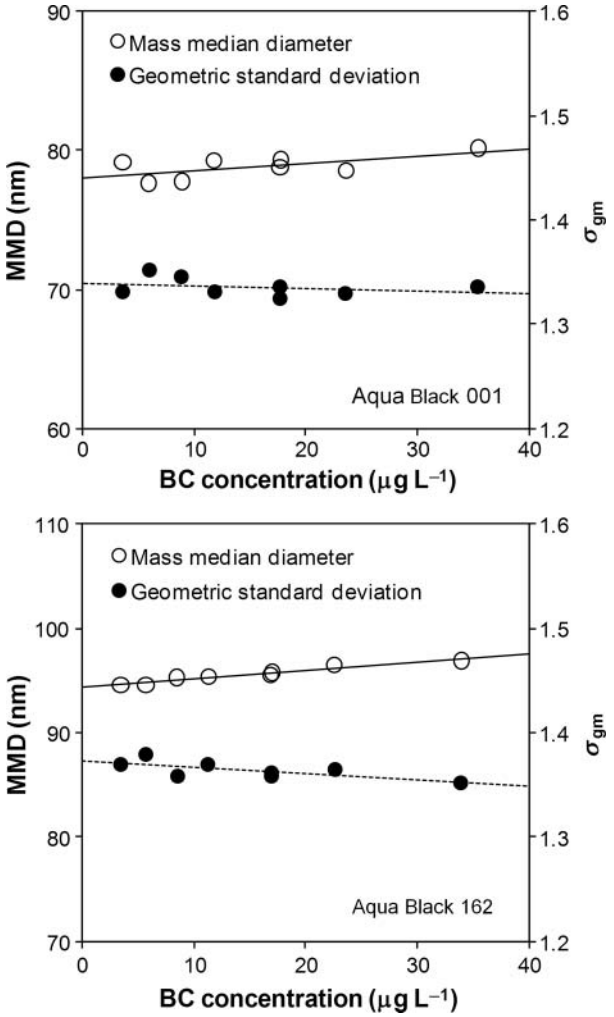

FIG. 11. Mass median diameter (MMD) and geometric standard deviation (σ_{gm}) of Aqua Black 001 and Aqua Black 162 versus the BC concentration in water. The solid and dashed lines indicate linear fitting to the MMD and σ_{gm}, respectively.

5.2. Rainwater

Third, we assessed the effect of coagulation for BC in rainwater, using the sample collected in Tokyo on December 21, 2010. This is the same sample used for the assessment of the effect of water-soluble species on the efficiency, discussed in Section 3.2. The BC concentration in this sample was measured to be 208 μg L^{-1}. We diluted this sample with pure water in order to generate different BC concentrations in water. It should be noted that the concentrations of the other water-soluble species were diluted as well.

Figure 12 shows the normalized number and mass size distributions for BC mass concentrations of 208 (undiluted) and 35 μg L^{-1} (diluted).

TABLE 3
Slopes and correlation coefficients (R^2) of the fitted lines to MMD and σ_{gm} shown in Figures 11, 12, 15, and 16

Sample name	Slope for MMD [nm (μg L^{-1})$^{-1}$]	R^2 for MMD	Slope for σ_{gm} [(μg L^{-1})$^{-1}$]	R^2 for σ_{gm}
AB-001	5.1×10^{-2}	0.40	-2.5×10^{-4}	0.09
AB-162	7.9×10^{-2}	0.94	-6.0×10^{-4}	0.49
BC in rainwater	7.7×10^{-2}	0.76	-6.8×10^{-4}	0.92
BC in rainwater	1.7×10^{-1} (for CMD)	0.86 (for CMD)	-4.6×10^{-4} (for σ_{gc})	0.32 (for σ_{gc})

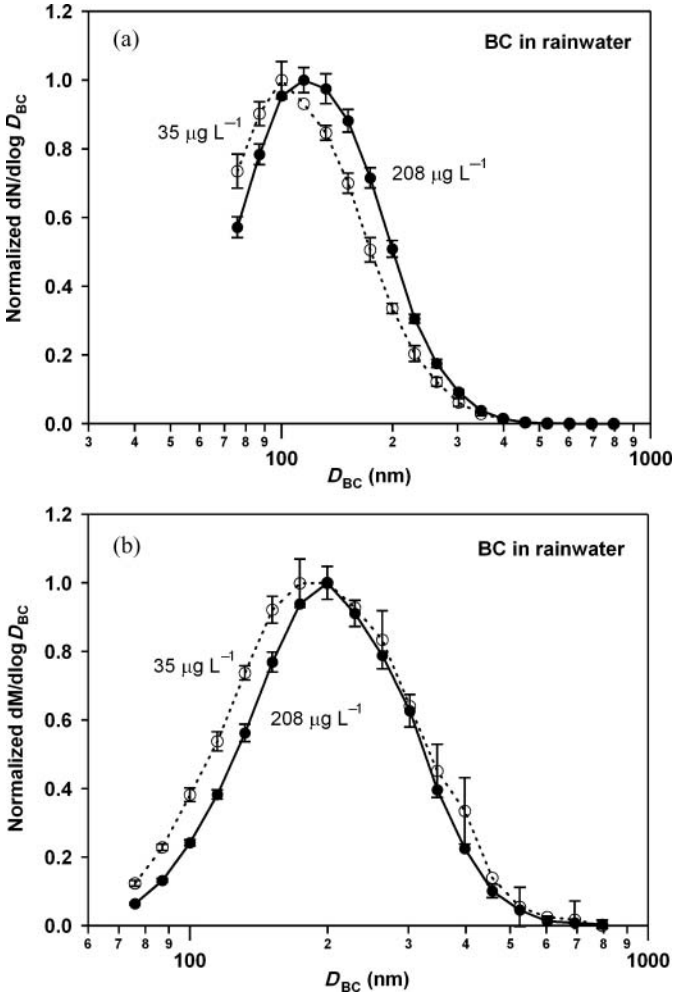

FIG. 12. (a) Normalized number and (b) mass size distributions of BC in original rainwater (208 μg L^{-1}) and in diluted rainwater (35 μg L^{-1}). Error bars show 1 σ values. Some error bars were removed for clarity.

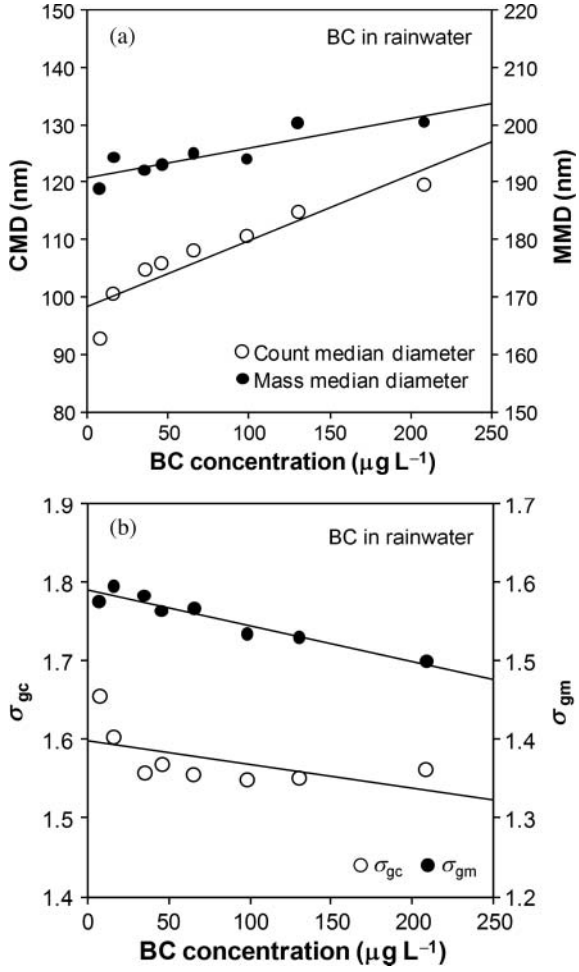

FIG. 13. (a) CMD and MMD and (b) σ_{gc} and σ_{gm} of BC in diluted rainwater versus the BC concentrations in rainwater. Solid lines indicate linear fitting.

Each size distribution was fitted by a lognormal function (fitted functions are not shown in Figure 12). The fitting errors in deriving the CMD and MMD were less than 1 and 3 nm, respectively. Figure 13 shows the dependencies of CMD, MMD, σ_{gc}, and σ_{gm} on BC concentration.

CMD and MMD increased and σ_{gc} and σ_{gm} decreased with the increase in BC concentration. The observed changes in MMD and σ_{gm} are qualitatively consistent with the results using AB-001 and AB-162. For quantitative comparison, Table 3 summarizes the slopes of the MMD and σ_{gm} (and also CMD and σ_{gc} for BC in rainwater) correlations with BC concentration, together with their correlation coefficients (R^2). The slopes of the MMD and σ_{gm} for BC in rainwater were close to those of AB-162. However, the slopes for AB-001 were significantly different, likely due to the larger uncertainties in the determinations of MMD and σ_{gm}.

Microphysical properties, including particle shape and solubility in water, are considerably different between BC in rainwater and AB-162. The present result indicates that the physical processes of coagulation of BC upon evaporation of water droplets are not sensitive to the microphysical properties of BC.

The results presented in this section have provided a good basis for interpreting the apparent changes in the size distributions of BC in rainwater in terms of coagulation processes, which are insensitive to the microphysical properties of BC. The best estimate of the CMD, MMD, σ_{gc}, and σ_{gm} of BC in rainwater

TABLE 4
BC size distribution in rainwater collected in Tokyo in December 2010 and average BC size distribution in ambient air in Tokyo in August and September 2009

Sample name	CMD (nm)	σ_{gn}	MMD (nm)	σ_{gm}
BC in rainwater	98	1.60	191	1.59
BC in ambient air	64	1.66	146	1.82

TABLE 5
BC concentrations and size distributions in rainwater along with rain rate on December 11, 2009, at the University of Tokyo campus

December 11, 2009 (LT)	Rain duration (h)	Rain amount (mm)	Rain rate (mm h^{-1})	BC concentration ($\mu g\ L^{-1}$)
No. 1 (0945–1325)	3.67	6.0	1.63	123
No. 2 (1350–1550)	2.00	3.5	1.75	51
No. 3 (1550–1750)	2.00	4.5	2.25	16
No. 4 (1750–1950)	2.00	8.0	4.00	7
No. 5 (1950–2150)	2.00	5.5	2.75	8
No. 6 (2150–2250)	1.00	1.0	1.00	15
Total	12.67	28.5	2.25	39

Note: LT, local time.

can be obtained by linear extrapolation of the data to the limit of zero BC concentration (Figure 13).

6. CORRECTED BC SIZE DISTRIBUTION IN RAINWATER

We estimated the CMD, MMD, σ_{gc}, and σ_{gm} of the BC size distribution in rainwater by linear extrapolation of correlation plots to the limit of zero BC concentration in Figure 13. The corrected values are summarized in Table 4.

The BC size distributions in ambient air in Tokyo were measured by the same SP2 in August and September in 2009 (Kondo et al. 2011a). The average values of CMD, MMD, σ_{gc} and σ_{gm} for these observations are also given in Table 4 for comparison. The CMD and MMD of BC in rainwater were larger than those in ambient air by 34 and 45 nm, although they were measured in different seasons.

As another example of field measurement by this system, the concentrations of BC in rainwater during one rain event in December 2009 are summarized in Table 5.

Higher BC concentrations were measured at earlier stages of the rain event, and the mean concentration was 39 $\mu g\ L^{-1}$. This is a demonstration of the advantage of the highly time-resolved measurements enabled by the present system.

7. SUMMARY AND CONCLUSION

We evaluated a method to measure accurately the concentration and size distribution of BC particles suspended in rainwater. Rainwater samples were aerosolized by an ultrasonic nebulizer. BC particles were extracted by drying the generated water droplets. The mass of each BC particle was then measured by a well-calibrated SP2, based on the LII technique. The volume of a rainwater sample required for BC measurement was less than 5 mL.

The overall efficiency of extracting BC particles from rainwater was determined by using AB-162 dissolved in pure water as a function of the pump liquid flow rate and BC concentration. The efficiency was measured to be 11.4% ± 0.83% at a liquid flow rate of 3.16 $L\ s^{-1}$ depending little on the BC concentration. The efficiency was stable to factor-of-10 changes in the concentration of water-soluble species in rainwater samples. This demonstrates the nondetectable effect of water-soluble species on the efficiency in these samples. The total uncertainty of the measurement of BC concentration in rainwater was estimated to be ±20%. Storage of rainwater for 50 days in a refrigerator caused changes in the BC mass concentration of less than 14%.

The effect of coagulation upon extraction of BC was evaluated by changing the concentrations of AB-162 in pure water and BC in rainwater. The MMD increased and σ_{gm} decreased with the increase in BC. Notably the slopes and the correlations of these parameters with BC concentrations were similar for AB-162 and BC in rainwater, despite large differences in their microphysical properties. This provides a strong basis in making corrections to CMD, MMD, σ_{gc}, and σ_{gm} based on the measured slope. In addition, this gives support in using the extraction efficiency of AB-162 for the analysis of BC in rainwater because the same physical processes are involved in controlling these parameters.

We estimated the concentration and size distribution of BC in a rainwater sample collected in Tokyo in December 2010. The BC concentration was 208 $\mu g\ L^{-1}$ and the BC size distribution was approximated by lognormal distribution functions with a CMD and MMD of 98 and 191 nm, respectively. We successfully applied this method to time-resolved measurements of BC in rainwater during one rain event in Tokyo in December 2009. Higher BC concentrations were measured at earlier stages of the rain event.

REFERENCES

Cerqueira, M., Pio, C., Legrand, M., Puxbaum, H., Kasper-Giebl, A., Afonso, J., Preunkert, S., Gelencsér, A., and Fialho, P. (2010). Particulate Carbon in Precipitation at European Background Sites. *J. Aerosol Sci.*, 41:51–61.

Chylek, P., Kou, L., Johnson, B., Boudala, F., and Lesins, G. (1999). Black Carbon Concentrations in Precipitation and Near Surface Air in and near Halifax, Nova Scotia, *Atmos. Environ.*, 33:2269–2277.

Clarke, A. D., and Noone, K. J. (1985). Soot in The Arctic Snowpack: A Cause for Perturbations in Radiative Transfer. *Atmos. Environ.*, 19:2045–2053.

Ducret, J., and Cachier, H. (1992). Particulate Carbon Content in Rain at Various Temperate and Tropical Locations. *J. Atmos. Chem.*, 15:55–67.

Dusek, U., Reischl, G. P., and Hitzenberger, R. (2006). CCN Activation of Pure Coated Carbon Black Particles. *Environ. Sci. Technol.*, 40:1223–1230.

Facchini, M. C., Decesari, S., Mircea, M., Fuzzi, S., and Loglio, G. (2000). Surface Tension of Atmospheric Wet Aerosol and Cloud/Fog Droplets in Relation to Their Organic Carbon Content and Chemical Composition. *Atmos. Environ.*, 34:4853–4857.

Flanner, M. G., Zender, C. S., Hess, P. G., Mahowald, N. M., Painter, T. H., Ramanathan, V., and Rasch, P. J. (2009). Springtime Warming and Reduced Snow Cover from Carbonaceous Particles. *Atmos. Chem. Phys.*, 9:2481–2497.

Flanner, M. G., Zender, C. S., Randerson, J. T., and Rasch, P. J. (2007). Present-Day Climate Forcing and Response from Black Carbon in Snow. *J. Geophys. Res.*, 112:D11202, doi: 10.1029/2006JD008003.

Hadley, O. L., Corrigan, C. E., and Kirchstetter, T. W. (2008). Modified Thermal-Optical Analysis Using Spectral Absorption Selectivity to Distinguish Black Carbon from Pyrolized Organic Carbon. *Environ. Sci. Technol.*, 42:8459–8464.

Hansen, J., and Nazarenko, L. (2004). Soot Climate Forcing via Snow and Ice Albedos. *Proc. Natl. Acad. Sci.,* 101:423–428.

Hoenig, M., Docekalova, H., and Baeten, H. (2000). Additional Considerations for Trace Element Analysis of Environmental Matrices Using Inductively Coupled Plasma Atomic Emission Spectrometry with Ultrasonic Nebulization. *Analusis*, 28:419–425.

IPCC. (2007). *Climate Change 2007: The Physical Science Basis. Contribution of Working Group I to the 4th Assessment Report of the IPCC*. Cambridge University Press, Cambridge, UK, p. 160–171, Ch. 2.

Jacobson, M. Z. (2001). Strong Radiative Heating Due to the Mixing State of Black Carbon in Atmospheric Aerosols. *Nature*., 409:695–697.

Kajino, M., and Kondo, Y. (2011). EMTACS: Development and Regional-Scale Simulation of a Size, Chemical, Mixing State and Shape Resolved Atmospheric Particle Model. *J. Geophys. Res.*, 116:D02303, doi: 10.1029/2010JD015030.

Kiss, G., Tombacz, E., and Hansson, H. (2005). Surface Tension Effects of Humic-Like Substances in the Aqueous Extract of Tropospheric Fine Aerosol. *J. Atmos. Chem.*, 50:279–294.

Kondo, Y., Matsui, H., Moteki, N., Sahu, L., Takegawa, N., Kajino, M., Zhao, Y., Cubison, M. J., Jimenez, J. L., Vay, S., Diskin, G. S., Anderson, B., Wisthaler, A., Mikoviny, T., Fuelberg, H. E., Blake, D. R., Huey, G., Weinheimer, A. J., Knapp, J. D., and Brune, H. (2011b). Emissions of Black Carbon, Organic, and Inorganic Aerosols from Biomass Burning in North America and Asia in 2008. *J. Geophys. Res.*, 116: D08204, doi: 10.1029/2010JD015152.

Kondo, Y., Sahu, L., Moteki, N., Khan, F., Takegawa, N., Liu, X., Koike, M., and Miyakawa, T. (2011a). Consistency and Traceability of Black Carbon Measurements Made by Laser-Induced Incandescence, Thermal-Optical Transmittance, and Filter-Based Photo-Absorption Techniques. *Aerosol Sci. Technol.*, 45:295–312.

Kuwata, M., Kondo, Y., Mochida, M., Takegawa, N., and Kawamurra, K. (2007). Dependence of CCN Activity of Less Volatile Particles on the Amount of Coating Observed in Tokyo. *J. Geophys. Res.*, 112:D11207, doi: 10.1029/2006JD007758.

Kuwata, M., Kondo, Y., and Takegawa, N. (2009). Critical Condensed Mass for Activation of Black Carbon as Cloud Condensation Nuclei. *J. Geophys. Res.*, 114:D20202, doi: 10.1029/2009JD012086.

Matsui, H., Kondo, Y., Moteki, N., Takegawa, N., Sahu, L. K., Zhao, Y., Fuelberg, H. E., Sessions, W. R., Diskin, G., Blake, D. R., Wisthaler, A., and Koike, M. (2011). Seasonal Variation of the Transport of Black Carbon Aerosol from the Asian Continent to the Arctic During the ARCTAS Aircraft Campaign. *J. Geophys. Res.*, 116: D05202, doi: 10.1029/2010JD015067.

McConnell, J. R., Edwards, R., Kok, G. L., Flanner, M. G., Zender, C. S., Saltzman, E. S., Banta, J. R., Pasteris, D. R., Carter, M. M., and Kahl, J. D. W. (2007). 20th-Century Industrial Black Carbon Emissions Altered Arctic Climate Forcing. *Science*, 317:1381–1384.

Miyazaki, Y., Kondo, Y., Takegawa, N., Komazaki, Y., Fukuda, M., Kawamura, K., Mochida, M., Okuzawa, K., and Weber, R. J. (2006). Time-Resolved Measurements of Water-Soluble Organic Carbon in Tokyo. *J. Geophys. Res.*, 111:D23206, doi: 10.1029/2006JD007125.

Moteki, N., and Kondo, Y. (2007). Effects of Mixing State on Black Carbon Measurement by Laser-Induced Incandescence. *Aerosol Sci. Technol.*, 41:398–417.

Moteki, N., and Kondo, Y. (2010). Dependence of Laser-induced Incandescence on Physical Properties of Black Carbon Aerosols: Measurements and Theoretical Interpretation. *Aerosol Sci. Technol.*, 44:663–675.

Ogren, J. A., and Charlson, R. J. (1983). Determination of Elemental Carbon in Rainwater. *Anal. Chem.*, 55:1569–1572.

Ogren, J. A., Groblicki, P. J., and Charlson, R. J. (1984). Measurement of the Removal Rate of Elemental Carbon from the Atmosphere. *Sci. Tot. Environ.*, 36:329–338.

Okuda, T., Iwase, T., Ueda, H., Suda, Y., Tanaka, S., Dokiya, Y., Fushimi, K., and Hosoe, M. (2005). Long-Term Trend of Chemical Constituents in Precipitation in Tokyo Metropolitan Area, Japan, from 1990 to 2002. *Sci. Tot. Environ.*, 339:127–141.

Ramanathan, V., Ramana, M. V., Roberts, G., Kim, D., Corrigan, C., Chung, C., and Winker, D. (2007). Warming Trends in Asia Amplified by Brown Cloud Solar Absorption. *Nature*, 448:575–579.

Seinfeld, J. H., and Pandis, S. N. (2006). *Atmospheric Chemistry and Physics*. John Wiley & Sons, New York, pp. 949–953, Chapter 20.

Sempere, R., and Kawamura, K. (1994). Comparative Distributions of Dicarboxylic Acids and Related Polar Compounds in Snow, Rain and Aerosols from Urban Atmosphere. *Atmos. Environ.*, 28:449–459.

Slinn, W. G. N. (1983). *Precipitation Scavenging, in Atmospheric Sciences and Power Production—1979*. Division of Biomedical Environmental Research, US Department of Energy, Washington, DC, Chapter 11, p. 466–532.

Stier, P., Feichter, J., Kinne, S., Kloster, S., Vignati, E., Wilson, J., Ganzeveld, L., Tegen, I., Werner, M., Balkanski, Y., Schulz, M., Boucher, O., Minikin, A., and Petzold, A. (2005). The Aerosol-Climate Model ECHAM5-HAM. *Atmos. Chem. Phys.*, 5:1125–1156.

Stier, P., Seinfeld, J. H., Kinne, S., Feichter, J., and Boucher, O. (2006). Impact of Nonabsorbing Anthropogenic Aerosols on Clear-Sky Atmospheric Absorption. *J. Geophys. Res.*, 111:D18201, doi: 10.1029/2006JD007147.

Svenningsson, B., Rissler, J., Swietlicki, E., Mircea, M., Bilde, M., Facchini, M. C., Decesari, S., Fuzzi, S., Zhou, J., Monster, J., and Rosenorn, T. (2006). Hygroscopic Growth and Critical Supersaturations for Mixed Aerosol Particles of Inorganic and Organic Compounds of Atmospheric Relevance. *Atmos. Chem. Phys.*, 6:1937–1952.

Waite, D. A., and Ramsden, D. (1971). The Production of Experimentally Labeled Aerosols in the Sub-Micron Range. *Aerosol Sci.*, 2:425–436.

Warren, S. G., and Wiscombe, W. J. (1980). A Model for the Spectral Albedo of Snow, II, Snow Containing Atmospheric Aerosols. *J. Atmos. Sci.*, 37:2734–2745.

Willey, J. D., Kieber, R. J., Eyman, M. S., and Avery, Jr., G. B. (2000). Rainwater Dissolved Organic Carbon: Concentrations and Global Flux. *Global Biogeochem. Cycles*, 14:139–148.